

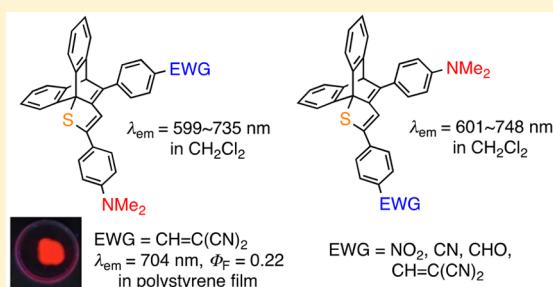
Red and Near-Infrared Photoluminescence of D- π -A-Type Compounds Based on a 1,4-Diaryl-1-thio-1,3-butadiene Conjugated System in a Dibenzobarrelene Skeleton

Akihiko Ishii,* Yukihiro Makishima, and Norio Nakata

Department of Chemistry, Graduate School of Science and Engineering, Saitama University, 255 Shimo-okubo, Sakura-ku, Saitama 338-8570, Japan

Supporting Information

ABSTRACT: 1,4-Diaryl-1-thio-1,3-butadiene derivatives having a π -donor dimethylamino group and several π -acceptor substituents at both terminals of the conjugated system were synthesized by intramolecular [4 + 2] cycloaddition of 1-thio-enynes and subsequent chemical transformations. They displayed largely red-shifted absorption and emission spectra in solution, the powder state, and in polymer films. The derivatives with a 2,2-dicyanoethenyl group as the π -acceptor exhibited inverted solvatochromism in both optical absorption and fluorescence spectroscopies.



Compounds that emit red and near-infrared (NIR) light have been attracting considerable attention from the viewpoint of applications of fluorescence imaging in biological study^{1,2} and of functional materials for optoelectronic devices.^{3–5} To improve red and NIR emissions, an effective method is the introduction of π -donor and π -acceptor substituents into a π -conjugated system (D- π -A conjugated system), which leads to an intramolecular charge transfer upon photoexcitation. Up to now, large bathochromic shifts of fluorescence have been observed.⁴ However, there still remain problems in improving photostability and the fluorescence quantum yield in the solid state.^{1e,2e} There are only a few examples in the solid state of emission maxima of over 700 nm with efficient quantum yields.⁴

Swager and co-workers have studied for decades the photophysical features of iptycenes represented by triptycene.⁶ Yang and co-workers recently discussed the effects of iptycene scaffolds on the photoluminescent properties of D- π -A-type 4-aminobenzonitriles from the viewpoint of the steric effects on solvation and the twist angles of the amino groups, as well as the hyperconjugation between the peripheral phenylene groups with the core π -system.⁷ Recently, we have developed highly fluorescent compounds **1** that contain 1-thio- and 1-seleno-1,3-butadiene conjugated systems as fluorophores secured in a rigid dibenzobarrelene skeleton (Figure 1).⁸ We have also reported 4-aza⁹ and thiophene-fused¹⁰ derivatives and phosphorescent chalcogenplatinacycles fused with dibenzobarrelene or triptycene,¹¹ indicating that rigid and bulky iptycene skeletons can play important roles regarding their photoluminescent properties.^{6,7,12} In this study, we demonstrate the development of red and NIR light emitters with efficient quantum yields in solution and in solid states by constructing D- π -A conjugated systems based on 1,4-diphenyl-1-thio derivative **2**. Some compounds are

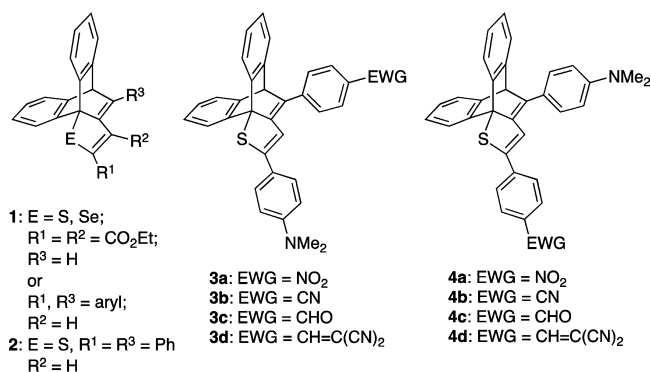


Figure 1. Structures of 1-thio- or 1-seleno-1,3-butadiene derivatives **1–4**.

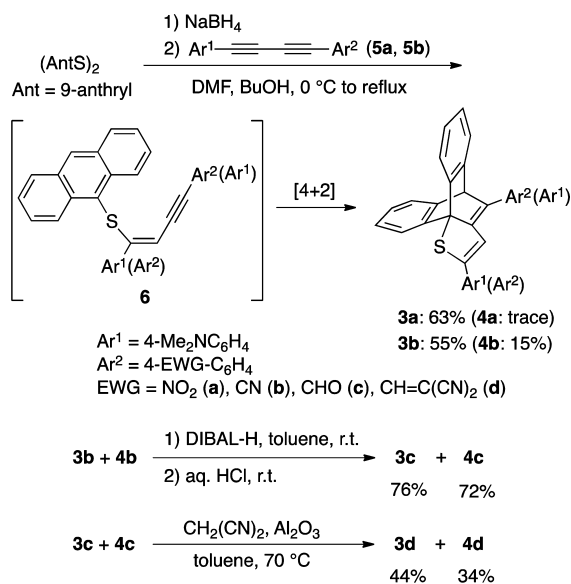
found to exhibit NIR emissions in polymer films with high efficiency.

We employed the NMe₂ group as the π -donor and NO₂ (a), CN (b), CHO (c), and CH=C(CN)₂ (d) groups as the π -acceptors for the D- π -A conjugated systems (**3** and **4**, Figure 1). The target compounds **3** and **4** were synthesized as depicted in Scheme 1. The reaction of AntS⁻ (Ant = 9-anthryl), prepared in situ by the reduction of (AntS)₂ with NaBH₄, with diyne **5a** or **5b**, produced two regioisomers **3a** and **4a** or **3b** and **4b**, respectively, through intramolecular [4 + 2] cycloadditions of intermediates **6**.⁶ In the syntheses, **3a** and **3b** were the major products, and in the case of the nitro derivatives, only a trace amount of compound assignable as **4a** was detected in the ¹H NMR spectrum of the reaction mixture. Formyl derivatives **3c**

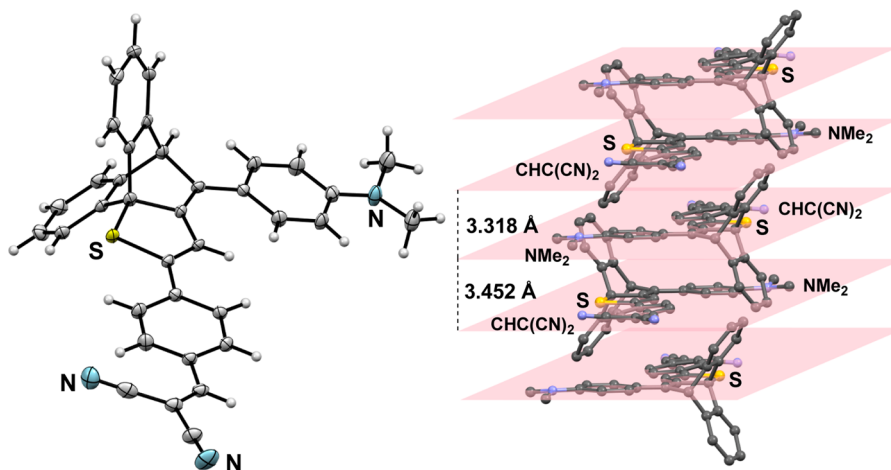
Received: September 18, 2015

Published: November 2, 2015

Scheme 1. Synthesis of 3 and 4



and **4c** were synthesized by the reduction of a mixture of cyano derivatives **3b** and **4b** with DIBAL-H, followed by hydrolysis under acidic conditions. 2,2-Dicyanoethenyl derivatives **3d** and **4d** were synthesized by treatment of a mixture of **3c** and **4c** with dicyanomethane in the presence of Al_2O_3 .¹³ The regioisomers were separated by silica-gel column chromatography. Their structures were determined by spectroscopic means and X-ray crystallography. Figure 2 exhibits an ORTEP drawing of **4d** (see the Supporting Information for others, Figures S1–S6). The two terminal aryl groups in **4d** possess high planarity to the 1-thio-1,3-butadiene conjugated system, forming a pseudoplane. As shown in Figure 2 (right), due to the π - π -stacking of the pseudoplanes in a head-to-tail manner, **4d** forms a somewhat slipped column structure with alternate mean-plane distances of 3.318 and 3.452 Å. This type of π - π stacking in a head-tail manner is unique for **4d** in **3a–d** and **4b–d**. The torsion angles of $\text{C}_6\text{H}_4\text{NMe}_2$ and $\text{C}_6\text{H}_4\text{CH}=\text{C}(\text{CN})_2$ groups are $6.9(5)^\circ$ and $4.5(5)^\circ$, respectively, the latter of which is remarkably small compared with those of the others ($30.2(3)$ – $45.1(3)^\circ$) (see the Supporting Information, Tables S1–S7).

Figure 2. ORTEP drawing of **4d** (left) and a part of the packing structure (right).

Photophysical properties of **3** and **4** in CH_2Cl_2 are summarized in Table 1 together with the corresponding data

Table 1. Photophysical Properties of **3** and **4** in CH_2Cl_2 ^a

compound	λ_{abs} (ϵ)/nm ($/\text{M}^{-1} \text{cm}^{-1}$)	λ_{em} / nm	Stokes shift/ cm^{-1} (nm)	Φ_{F} ^b
3a	484 (20000)	625	4600 (141)	0.003
3b	436 (29000)	599	6200 (163)	0.42
4b	451 (20000)	601	5500 (150)	0.76
3c	449 (27000)	616	6000 (167)	0.46
4c	464 (16000)	645	6000 (181)	0.54
3d	543 (12000)	735	4800 (192)	0.06
4d	558 (25000)	748	4600 (190)	0.01
2	378 (23000)	491	6100 (113)	1.0

^a 1×10^{-5} M in CH_2Cl_2 at room temperature. ^bAbsolute emission quantum yields determined with a calibrated integrating sphere system.

of **2** for reference. The long-wavelength absorption maxima of **3** and **4** are largely red-shifted by 58–180 nm compared with that of **2** ($\lambda_{\text{abs}} = 378$ nm) (Figure 3, left). The emission spectra also exhibit large red shifts (Figure 3, right). In particular, the emission maxima (λ_{em}) of 2,2-dicyanoethenyl derivatives **3d** and **4d** reached the NIR region, 735 and 748 nm, respectively, which is evidence of a red shift of ca. 250 nm from that of **2** ($\lambda_{\text{em}} = 491$ nm). These bathochromic shifts in the optical absorption and emission spectra indicate that the conjugations are effectively extended by π -donor and π -acceptor substituents introduced at both terminals of **2**. The fluorescence quantum yields (Φ_{F}) of **3b**, **4b**, **3c**, and **4c** are moderate to high (0.42–0.76). **3d** and **4d** have low Φ_{F} values down to 0.06 and 0.01, respectively. Φ_{F} of **3a** decreased to 0.003. Similar fluorescence quenching of nitro compounds has been reported.¹⁴

Solvent effects on the photophysical properties of **3b–d** and **4b–d** were investigated.¹⁵ In cases of compounds having CN (**b**) or CHO (**c**) as the π -acceptor, whereas the solvent effects on long-wavelength absorption were rather small, large bathochromic shifts of emission (73 (**3b**), 108 (**4b**), 81 (**3c**), and 138 (**4c**) nm) were observed with the increase of the solvent polarity from hexane to MeCN (see the Supporting Information, Figures S8–S11 and Tables S8–S11). This positive solvatochromism of emission suggests that their excited states are stabilized by solvation in polar solvents.

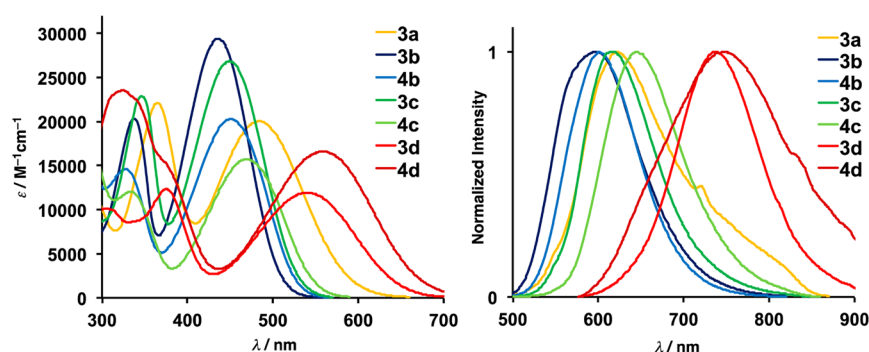


Figure 3. Absorption (left) and fluorescence (right) spectra of 3 and 4 in CH_2Cl_2 .

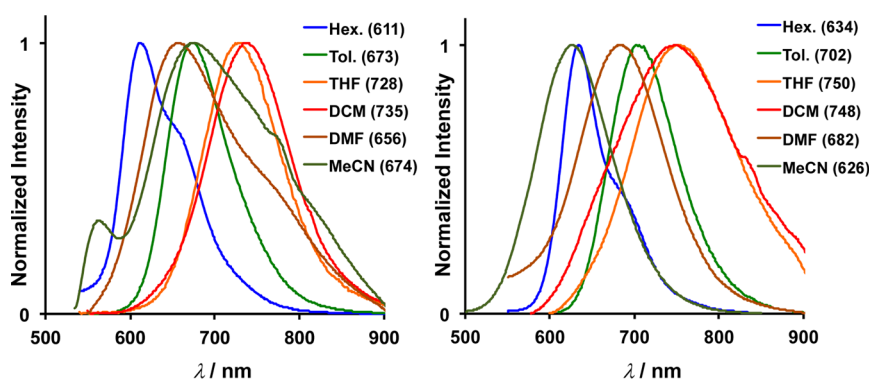


Figure 4. Optical absorption and fluorescence spectra of **3d** (left) and **4d** (right) in several solvents. λ_{em} /nm values are given in parentheses.

The photoluminescent color of the formyl derivative **4c** changes dramatically from yellowish green in hexane ($\lambda_{\text{em}} = 531$ nm, $\Phi_{\text{F}} = 1.0$) and orange in toluene ($\lambda_{\text{em}} = 584$ nm, $\Phi_{\text{F}} = 0.92$) to red in MeCN ($\lambda_{\text{em}} = 669$ nm, $\Phi_{\text{F}} = 0.36$) (see the Supporting Information, Figure S11). As a result, Stokes shifts become larger with the increase of solvent polarity to lead to good linear correlations in Lippert–Mataga plots for **3b**, **4b**, **3c**, and **4c** (see the Supporting Information, Figure S14).¹⁶

Interestingly, in the cases of **3d** and **4d**, their long-wavelength absorptions and emissions displayed inverted solvatochromism¹⁷ (see the Supporting Information, Tables S12 and S13 and Figures S12 and S13 for optical absorption spectra). Long-wavelength absorptions of **3d** and **4d** showed positive solvatochromism from hexane to CHCl_3 (30 and 25 nm, respectively) and then negative solvatochromism from CHCl_3 to MeCN (−36 and −35 nm, respectively). Inverted solvatochromism has been discussed on several types of betaine dyes¹⁸ and D- π -A-type compounds¹⁹ for decades, and the origin has been presumed to be the change of the ground-state electronic state.¹⁷ This seems to be the present case, implying the increase of the contribution of charge-separated resonance structures in their ground states in polar solvents. The magnitude of the inverted solvatochromism of **3d** and **4d** for optical absorption is rather smaller than those of the betaine dyes¹⁸ and comparable to those of reported D- π -A-type compounds.¹⁹

As for emissions of **3d** and **4d**, much larger inverted solvatochromisms were observed. Figure 4 shows the emission spectra of **3d** and **4d**; red shifts from hexane to CH_2Cl_2 (124 nm for **3d**) or THF (116 nm for **4d**) and then blue shifts from CH_2Cl_2 to DMF (79 nm for **3d**) and from THF to MeCN (124 nm for **4d**). Their emission maxima in THF were observed in the NIR region ($\lambda_{\text{em}} = 728$ nm for **3d** and 750 nm

for **4d**) with more than 110 nm red shifts from those in hexane. In particular, λ_{em} of **4d** was 702 nm in toluene with a relatively high quantum yield ($\Phi_{\text{F}} = 0.23$). It has been reported that the emission of 2-(2,2-dicyanoethenyl)-7-(dimethylamino)-9,9-diethylfluorene showed a positive solvatochromism shifting from 528 nm in cyclohexane to 711 nm in DMSO.¹³ The fluorene derivative and **3d** and **4d** have the same π -donor and π -acceptor substituents, and it seems that their different solvatochromic behaviors are attributed to the longer conjugated systems of **3d** and **4d** than that of the fluorene derivative. Reports on the inverted solvatochromism of emission are limited; it was reported that 1-[4-(*N,N*-dimethylamino)phenyl]-4-(3-hydroxy-4-nitrophenyl)-3-(*E*)-buten-1-yne derivatives showed positive solvatochromism from heptane ($\lambda_{\text{em}} = 595$ nm) to CHCl_3 ($\lambda_{\text{em}} = 666$ nm) and negative solvatochromism from CHCl_3 to MeCN ($\lambda_{\text{em}} = 473$ nm) with low quantum yields ($\Phi_{\text{F}} = 0.082$ – 0.0014).²⁰ As far as we know, the compounds that exhibit inverted solvatochromism of both optical absorption and emission are quite rare.

HOMO and LUMO diagrams of **3d** and **4d** are depicted in Figure 5.²¹ The HOMO of **3d** locates on the $\text{Me}_2\text{NC}_6\text{H}_4\text{-C}(-\text{S})=\text{CH}-\text{CH}=\text{C}$ moiety mainly, and the LUMO locates on the $\text{C}_6\text{H}_4\text{CH}=\text{C}(\text{CN})_2$ moiety and the 1,3-butadiene conjugated system. This is also the case for **4d**. These diagrams of HOMO and LUMO indicate that the electronic excitation of **3d** and **4d** take place with intramolecular charge transfer. With respect to their HOMOs, **4d** has the linear conjugated system ($\text{S}-\text{C}=\text{CH}-\text{CH}=\text{C}-\text{C}_6\text{H}_4\text{NMe}_2$) that is longer than the cross-conjugated system of **3d** ($\text{Me}_2\text{NC}_6\text{H}_4-\text{C}(-\text{S})=\text{CH}-\text{CH}=\text{C}$), which would suggest the higher HOMO energy of **4d** than that of **3d**. In fact, the experimentally obtained HOMO level of **4d** (−4.94 eV) was higher by 0.09 eV than that of **3d** (−5.03 eV), and, on the other hand, the energy difference in

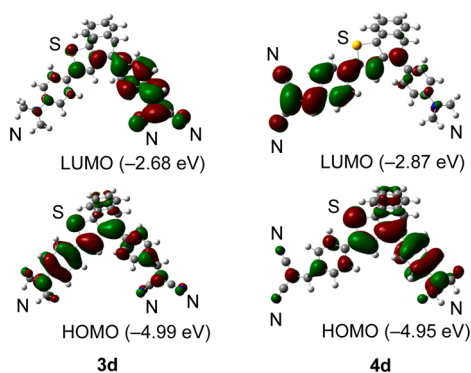


Figure 5. HOMO and LUMO diagrams of **3d** and **4d** obtained by DFT calculations at the B3LYP/6-31G(d) level.

LUMO levels, estimated from HOMO levels and HOMO–LUMO gaps, was rather small (–3.14 eV for **3d** and –3.11 eV for **4d**).²² A similar tendency was observed for other pairs of **3b** and **4b** and **3c** and **4c**.

Emission properties in the powder form and in polymer films are shown in Table 2. In the powder form, **3a–c** and **4b,c**

Table 2. Emission Properties in the Powder Form and in Polymer Films

compound	λ_{em} [nm] (Φ_F) ^a		
	powder	PMMA ^b	PS ^c
3a	653 (0.09)	641 (0.19)	644 (0.22)
3b	574 (0.44)	564 (0.26)	569 (0.37)
4b	619 (0.17)	579 (0.49)	565 (0.55)
3c	624 (0.13)	591 (0.15)	594 (0.21)
4c	640 (0.14)	609 (0.42)	598 (0.49)
3d	746 (0.02)	721 (0.12)	704 (0.22)
4d	n.e. (0.00)	688 (0.02)	722 (0.03)
2	483 (0.47)	484 (0.52)	483 (0.71)

^aAbsolute emission quantum yields determined with a calibrated integrating sphere system. ^bPoly(methyl methacrylate). ^cPoly(styrene).

showed the emissions in the range of 574–653 nm with lower-to-moderate quantum yields. **3d** exhibited a more red-shifted emission at 746 nm, being red-shifted by more than 263 nm from that of **2**. **4d**, possessing strong π – π stacks in the crystalline state, was found to be nonemissive. When dispersed in poly(styrene) (PS) film, **3a–c** and **4b,c** displayed emissions in the range from 565 to 644 nm, and **3d** and **4d** did in the NIR region (704 and 722 nm, respectively). These blue shifts (appearance of photoluminescence for **4d**), in contrast to those in the powder states, indicate that intermolecular interactions such as π – π stacking in the powder form, which contribute to lengthening of emission wavelengths and quenching of luminescence, are replaced by weaker intermolecular interactions with PS. The quantum yield of **3d** ($\Phi_F = 0.22$) is comparable to the highest value ever reported.⁴ In more polar poly(methyl methacrylate) (PMMA) films, **3a–d** and **4b–d** showed emissions at 564–721 nm with low-to-moderate quantum yields ($\Phi_F = 0.02$ –0.49). The stronger intermolecular interactions with PMMA led to red-shifted emissions for **4b**, **4c**, and **3d**, almost no changes for **2**, **3a**, **3b**, and **3c**, or a substantial blue shift for **4d**. The exceptional blue shift of **4d** seems to be a behavior similar to that observed in its negative solvatochrom-

ism in polar solvents. Photographs of **3d** in PMMA and PS films under irradiation at 365 nm are shown in Figure 6d.

In summary, we have presented that the dibenzobarrelene-based, D- π -A-type compounds **3** and **4** are materials that photoluminesce with red and NIR lights in a solution, the solid state, and in polymer films with good efficiencies. Compounds **3d** and **4d** with a 2,2-dicyanoethenyl group as the π -accepting group displayed the inverted solvatochromism on both optical absorption and emission in the range from nonpolar hexane to polar MeCN and DMF. The efficiency of the NIR emission of **3d** in the PS film is as high as those so far reported compounds that emit NIR light in the solid state. The red shifts of photoluminescence can be controlled by π -acceptors, and the CH=C(CN)₂ group is the most effective in this regard among those examined. Comparing regioisomers **3** and **4**, it was clarified experimentally and theoretically that isomer **4** has a smaller HOMO–LUMO gap than **3** does.

EXPERIMENTAL SECTION

General Procedures. All melting points were determined on a capillary tube apparatus and were uncorrected. ¹H and ¹³C NMR spectra were recorded on a 400 MHz spectrometer (400 MHz for ¹H and 100.6 MHz for ¹³C) using CDCl₃ as the solvent at room temperature. Absolute photoluminescence quantum yields were measured by a calibrated integrating sphere system. Solvents were dried by standard methods and freshly distilled prior to use. Column chromatography was performed with silica gel (70–230 mesh), and the eluent is shown in parentheses.

1-[p-(Dimethylamino)phenyl]-4-(p-nitrophenyl)-1,3-butadiyne (5a). A solution of 1-(bromoethynyl)-4-nitrobenzene (576.1 mg, 2.59 mmol) in MeOH (25 mL) was added to a mixture of 1-(dimethylamino)-4-ethynylbenzene (393.8 mg, 2.71 mmol), CuCl₂ (8.0 mg, 0.06 mmol), and NH₂OH·HCl (191.3 mg, 2.75 mmol) in BuNH₂ (6.2 mL) and MeOH (15 mL) at 0 °C under an argon atmosphere. After stirring for 6 h at 0 °C, the mixture was stirred at room temperature for 18 h, and then the precipitates were collected by filtration. The residue was washed with cold MeOH and then purified by column chromatography (hexane/CH₂Cl₂ = 1/1) to give **5a** (412.5 mg, 56%).

5a: Orange-red powder, mp 210–211 °C decomp (hexane/CH₂Cl₂). ¹H NMR (400 MHz, CDCl₃) δ 3.01 (s, 6H), 6.63 (d, $J = 7$ Hz, 2H), 7.42 (d, $J = 9$ Hz, 2H), 7.62 (d, $J = 9$ Hz, 2H), 8.19 (d, $J = 9$ Hz, 2H); ¹³C{¹H} NMR (101 MHz, CDCl₃) δ 40.0 (CH₃), 71.8 (C), 78.7 (C), 80.3 (C), 86.9 (C), 106.9 (C), 111.6 (CH), 123.6 (CH), 129.6 (C), 132.9 (CH), 134.1 (CH), 147.1 (C), 151.0 (C). Anal. Calcd for C₁₈H₁₄N₂O₂: C, 74.47; H, 4.86; N, 9.65. Found: C, 74.41; H, 4.82; N, 9.63.

1-[p-(Cyanophenyl)-4-[p-(dimethylamino)phenyl]-1,3-butadiyne (5b). A solution of 1-(bromoethynyl)-4-cyanobenzene (328.2 mg, 1.45 mmol) in MeOH (16 mL) was added to a mixture of 1-(dimethylamino)-4-ethynylbenzene (189.4 mg, 1.30 mmol), CuCl₂ (3.9 mg, 0.03 mmol), and NH₂OH·HCl (102.6 mg, 1.48 mmol) in BuNH₂ (3.1 mL) and MeOH (8 mL) at 0 °C under an argon atmosphere. After stirring for 6 h at 0 °C, the mixture was stirred at room temperature for 13 h, and then the precipitates were collected by filtration. The residue was washed with cold MeOH and then purified by column chromatography (hexane/CH₂Cl₂ = 1/1) to give **5b** (241.5 mg, 61%).

5b: Yellow powder, mp 190–191 °C (sublimation) (hexane/CH₂Cl₂). ¹H NMR (400 MHz, CDCl₃) δ 3.01 (s, 6H), 6.62 (d, $J = 9$ Hz, 2H), 7.41 (d, $J = 9$ Hz, 2H), 7.54 (d, $J = 9$ Hz, 2H), 7.60 (d, $J = 9$ Hz, 2H); ¹³C{¹H} NMR (101 MHz, CDCl₃) δ 40.0 (CH₃), 71.7 (C), 78.9 (C), 79.3 (C), 86.3 (C), 107.0 (C), 111.6 (CH), 111.7 (C), 118.4 (C), 127.6 (C), 132.0 (CH), 132.7 (CH), 134.0 (CH), 150.9 (C). Anal. Calcd for C₁₉H₁₄N₂: C, 84.42; H, 5.22; N, 10.36. Found: C, 83.93; H, 5.17; N, 10.29.

2-[p-(Dimethylamino)phenyl]-4-(p-nitrophenyl)-5H-5,9b[1',2']-benzenonaphtho[1,2-b]thiophene (3a). A solution of di(9-anthryl)

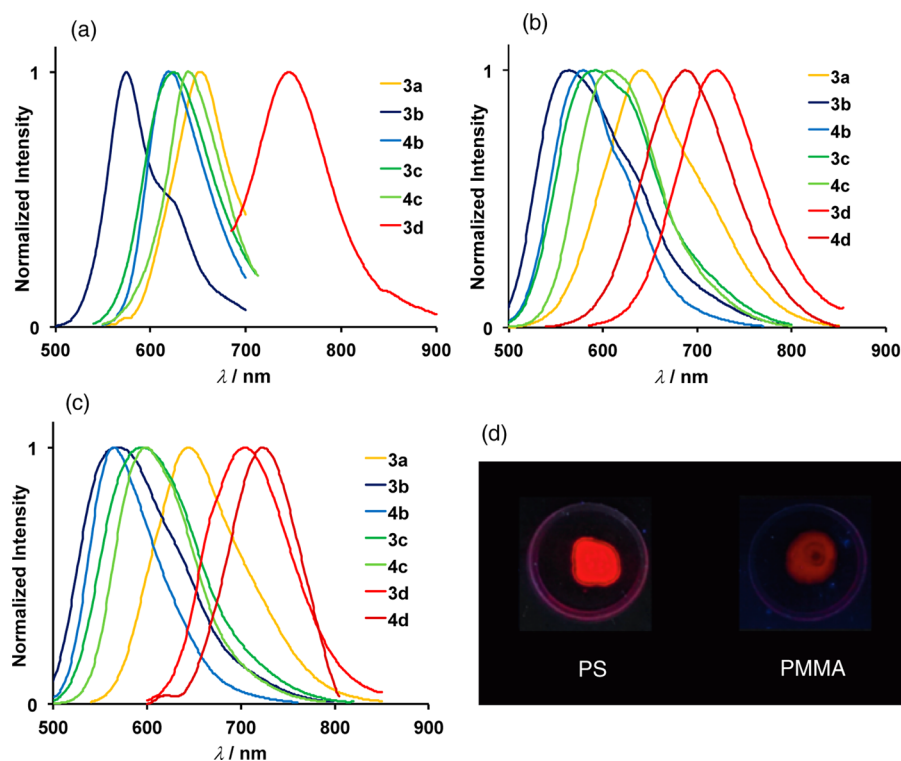


Figure 6. Fluorescence spectra of **3** and **4** in the powder form (a), in the PS film (b), and in the PMMA film (c). Photographs of **3d** dispersed in poly(styrene) (PS) and poly(methyl methacrylate) (PMMA) films under irradiation at 365 nm (d).

disulfide (78.3 mg, 0.19 mmol) in DMF (10 mL) was added slowly to a solution of NaBH_4 (20.3 mg, 0.34 mmol) in BuOH (25 mL) at 0 °C under an argon atmosphere. After stirring for 30 min at 0 °C, a solution of **5a** (100.0 mg, 0.34 mmol) in DMF (10 mL) was added to the mixture at 0 °C. The mixture was heated under reflux for 17 h, and then the reaction was quenched by addition of saturated aqueous NH_4Cl . The mixture was extracted with CH_2Cl_2 , and the extract was washed with water, dried over anhydrous Na_2SO_4 , and evaporated to dryness. The residue was subjected to column chromatography (hexane/ CH_2Cl_2 = 1/1) to give **3a** (106.7 mg, 63%).

3a: Dark red crystals, mp 255–256 °C decomp (hexane/ CH_2Cl_2). ^1H NMR (400 MHz, CDCl_3) δ 3.03 (s, 6H), 5.57 (s, 1H), 6.70 (s, 1H), 6.71 (d, J = 9 Hz, 2H), 7.06–7.11 (m, 4H), 7.41–7.43 (m, 2H), 7.53 (d, J = 9 Hz, 2H), 7.58 (d, J = 9 Hz, 2H), 7.58–7.62 (m, 2H), 8.21 (d, J = 9 Hz, 2H); $^{13}\text{C}\{^1\text{H}\}$ NMR (101 MHz, CDCl_3) δ 40.2 (CH_3), 55.7 (CH), 72.8 (C), 109.2 (CH), 111.8 (CH), 121.6 (C), 122.9 (CH), 123.9 (CH), 124.1 (CH), 125.6 (CH), 126.4 (CH), 126.7 (CH), 128.0 (CH), 133.0 (C), 142.7 (C), 145.54 (C), 145.57 (C), 145.63 (C), 151.3 (C), 154.0 (C), 158.6 (C). Anal. Calcd for $\text{C}_{32}\text{H}_{24}\text{N}_2\text{O}_2\text{S}$: C, 76.78; H, 4.83; N, 5.60. Found: C, 76.38; H, 4.73; N, 5.50.

2-[p-(Dimethylamino)phenyl]-4-(p-cyanophenyl)-5H-5,9b[1',2']-benzenonaphtho[1,2-b]thiophene (3b) and 2-(p-Cyanophenyl)-4-[p-(dimethylamino)phenyl]-5H-5,9b[1',2']-benzenonaphtho[1,2-b]thiophene (4b). A solution of di(9-anthryl) disulfide (253.3 mg, 0.55 mmol) in DMF (36 mL) was added slowly to a solution of NaBH_4 (50.0 mg, 1.32 mmol) in BuOH (40 mL) at 0 °C under an argon atmosphere. After stirring for 30 min at 0 °C, a solution of **5b** (297.4 mg, 1.10 mmol) in DMF (36 mL) was added to the mixture at 0 °C. The mixture was heated under reflux for 16 h, and then the reaction was quenched by addition of saturated aqueous NH_4Cl . The mixture was extracted with CH_2Cl_2 , and the extract was washed with water, dried over anhydrous Na_2SO_4 , and evaporated to dryness. The residue was subjected to column chromatography (hexane/ CH_2Cl_2 = 1/1) to give **3b** (292.1 mg, 55%) and **4b** (78.6 mg, 15%).

3b: Yellow crystals, mp 245–246 °C decomp (hexane/ CH_2Cl_2). ^1H NMR (400 MHz, CDCl_3) δ 3.03 (s, 6H), 5.53 (s, 1H), 6.66 (s, 1H), 6.71 (d, J = 9 Hz, 2H), 7.06–7.10 (m, 4H), 7.39–7.42 (m, 2H), 7.49

(d, J = 9 Hz, 2H), 7.57 (d, J = 9 Hz, 2H), 7.58–7.61 (m, 2H), 7.62 (d, J = 9 Hz, 2H); $^{13}\text{C}\{^1\text{H}\}$ NMR (101 MHz, CDCl_3) δ 40.2 (CH_3), 55.6 (CH), 72.6 (C), 109.2 (CH), 111.7 (CH), 119.2 (C), 121.7 (C), 122.9 (CH), 123.8 (CH), 125.5 (CH), 126.3 (CH), 126.8 (CH), 127.9 (CH), 132.3 (CH), 133.3 (C), 142.8 (C), 143.4 (C), 145.7 (C), 151.2 (C), 153.0 (C), 157.8 (C) (one quaternary carbon was not observed due to overlapping or broadening). Anal. Calcd for $\text{C}_{33}\text{H}_{24}\text{N}_2\text{S}$: C, 82.47; H, 5.03; N, 5.83. Found: C, 82.07; H, 4.97; N, 5.78.

4b: Orange crystals, mp 245–246 °C decomp (hexane/ CH_2Cl_2). ^1H NMR (400 MHz, CDCl_3) δ 2.99 (s, 6H), 5.56 (s, 1H), 6.74 (d, J = 9 Hz, 2H), 6.97 (s, 1H), 7.03–7.11 (m, 4H), 7.32 (d, J = 9 Hz, 2H), 7.41 (dd, J = 7, 2 Hz, 2H), 7.54 (dd, J = 7, 2 Hz, 2H), 7.65 (d, J = 9 Hz, 2H), 7.71 (d, J = 9 Hz, 2H); $^{13}\text{C}\{^1\text{H}\}$ NMR (101 MHz, CDCl_3) δ 40.4 (CH_3), 56.7 (CH), 72.3 (C), 111.2 (C), 112.3 (CH), 118.0 (CH), 118.8 (C), 123.2 (CH), 123.3 (CH), 125.4 (CH), 125.7 (C), 126.1 (CH), 126.6 (CH), 127.7 (CH), 132.3 (CH), 138.8 (C), 142.0 (C), 142.6 (C), 143.5 (C), 146.2 (C), 150.0 (C), 150.5 (C). Anal. Calcd for $\text{C}_{33}\text{H}_{24}\text{N}_2\text{S}$: C, 82.47; H, 5.03; N, 5.83. Found: C, 82.10; H, 4.96; N, 5.76.

2-[p-(Dimethylamino)phenyl]-4-(p-formylphenyl)-5H-5,9b[1',2']-benzenonaphtho[1,2-b]thiophene (3c) and 2-(p-Formylphenyl)-4-[p-(dimethylamino)phenyl]-5H-5,9b[1',2']-benzenonaphtho[1,2-b]thiophene (4c). A solution of DIBAL-H (1.02 M in hexane, 0.70 mL, 0.69 mmol) was added slowly to a mixture of **3b** and **4b** (220.1 mg, 0.46 mmol, **3b**:**4b** = 1:0.1) in toluene (4 mL) at 0 °C under an argon atmosphere. After stirring for 13 h at room temperature, CHCl_3 (20 mL) and 2 M HCl (5 mL) were added to the mixture. The mixture was stirred for 1 h at room temperature, and then the reaction was quenched by addition of saturated aqueous NaHCO_3 . The mixture was extracted with CH_2Cl_2 , and the extract was washed with water, dried over anhydrous Na_2SO_4 , and evaporated to dryness. The residue was subjected to column chromatography (hexane/ CH_2Cl_2 = 1/1) to give **3c** (153.2 mg, 76%) and **4c** (14.3 mg, 72%).

3c: Orange crystals, mp 220 °C decomp (hexane/ CH_2Cl_2). ^1H NMR (400 MHz, CDCl_3) δ 3.03 (s, 6H), 5.59 (s, 1H), 6.71 (d, J = 9 Hz, 2H), 6.72 (s, 1H), 7.05–7.11 (m, 4H), 7.40–7.45 (m, 2H), 7.56–7.61 (m, 6H), 7.86 (d, J = 9 Hz, 2H), 9.96 (s, 1H); $^{13}\text{C}\{^1\text{H}\}$ NMR (101 MHz, CDCl_3) δ 40.2 (CH_3), 55.7 (CH), 72.6 (C), 109.6 (CH),

111.7 (CH), 121.8 (C), 122.9 (CH), 123.8 (CH), 125.4 (CH), 126.3 (CH), 126.7 (CH), 127.9 (CH), 130.1 (CH), 134.0 (C), 134.1 (C), 142.9 (C), 145.1 (C), 145.8 (C), 151.1 (C), 152.6 (C), 157.6 (C), 191.5 (CH). Anal. Calcd for C₃₃H₂₅NOS: C, 81.96; H, 5.21; N, 2.90. Found: C, 81.55; H, 5.15; N, 2.79.

4c: Red-orange crystals, mp 220 °C decomp (hexane/CH₂Cl₂). ¹H NMR (400 MHz, CDCl₃) δ 2.99 (s, 6H), 5.57 (s, 1H), 6.74 (d, J = 8 Hz, 2H), 7.02 (s, 1H), 7.03–7.11 (m, 4H), 7.34 (d, J = 9 Hz, 2H), 7.41 (dd, J = 6, 1 Hz, 2H), 7.56 (dd, J = 6, 1 Hz, 2H), 7.78 (d, J = 8 Hz, 2H), 7.88 (d, J = 8 Hz, 2H), 10.00 (s, 1H); ¹³C{¹H} NMR (101 MHz, CDCl₃) δ 40.4 (CH₃), 56.7 (CH), 72.2 (C), 112.3 (CH), 117.9 (CH), 123.2 (CH), 123.3 (CH), 125.4 (CH), 125.8 (C), 126.1 (CH), 126.6 (CH), 127.7 (CH), 130.0 (CH), 135.6 (C), 140.2 (C), 141.7 (C), 142.7 (C), 144.3 (C), 146.3 (C), 149.9 (C), 150.7 (C), 191.4 (CH). Anal. Calcd for C₃₃H₂₅NOS: C, 81.96; H, 5.21; N, 2.90. Found: C, 81.45; H, 5.13; N, 2.79.

2-[p-(Dimethylamino)phenyl]-4-[p-(2,2-dicyanoethenyl)phenyl]-5H-5,9b[1',2']-benzenonaphtho[1,2-b]thiophene (3d) and 2-[p-(2,2-Dicyanoethenyl)phenyl]-4-[p-(dimethylamino)phenyl]-5H-5,9b[1',2']-benzenonaphtho[1,2-b]thiophene (4d). A suspension of **3c** and **4c** (200.6 mg, 0.41 mmol, **3c**:**4c** = 1:0.7), malononitrile (56.4 mg, 0.85 mmol), and alumina (195.7 mg) in toluene (3 mL) was stirred for 17 h at 70 °C under an argon atmosphere, and then the reaction was quenched by addition of saturated aqueous sodium chloride. The mixture was extracted with CH₂Cl₂, and the extract was washed with water, dried over anhydrous Na₂SO₄, and evaporated to dryness. The residue was subjected to column chromatography (hexane/CH₂Cl₂ = 1/1 to 1/2) to give **3d** (108.9 mg, 83%) and **4d** (78.7 mg, 87%).

3d: Dark purple crystals, mp 180–181 °C decomp (hexane/CH₂Cl₂). ¹H NMR (400 MHz, CDCl₃) δ 3.05 (s, 6H), 5.60 (s, 1H), 6.72 (d, J = 9 Hz, 2H), 6.77 (s, 1H), 7.06–7.12 (m, 4H), 7.40–7.44 (m, 2H), 7.56–7.62 (m, 6H), 7.66 (s, 1H), 7.90 (d, J = 9 Hz, 2H); ¹³C{¹H} NMR (101 MHz, CDCl₃) δ 40.2 (CH₃), 55.2 (CH), 72.9 (C), 80.0 (C), 109.6 (CH), 111.7 (CH), 113.3 (C), 114.4 (C), 121.6 (C), 122.9 (CH), 123.8 (CH), 125.6 (CH), 126.5 (CH), 126.9 (CH), 128.1 (CH), 128.5 (C), 131.3 (CH), 133.3 (C), 142.6 (C), 145.38 (C), 145.45 (C), 151.3 (C), 154.6 (C), 158.5 (CH), 159.2 (C). Anal. Calcd for C₃₆H₂₅N₃S·(H₂O)_{0.28}: C, 80.56; H, 4.80; N, 7.83. Found: C, 80.65; H, 4.67; N, 7.69 (The analytical sample was dried at 150 °C in vacuo for 3 days, but the amount (0.28) of H₂O still remained. The amount of H₂O was determined based on the ¹H NMR integral ratio of water against Me₄Si by comparing with that for the deuteriochloroform in the same bottle).

4d: Dark purple crystals, mp 242–243 °C decomp (hexane/CH₂Cl₂). ¹H NMR (400 MHz, CDCl₃) δ 3.00 (s, 6H), 5.58 (s, 1H), 6.74 (d, J = 9 Hz, 2H), 7.06 (s, 1H), 7.04–7.12 (m, 4H), 7.34 (d, J = 9 Hz, 2H), 7.42 (dd, J = 6, 2 Hz, 2H), 7.55 (dd, J = 6, 2 Hz, 2H), 7.66 (s, 1H), 7.75 (d, J = 8 Hz, 2H), 7.90 (d, J = 8 Hz, 2H); ¹³C{¹H} NMR (101 MHz, CDCl₃) δ 40.3 (CH₃), 56.7 (CH), 72.2 (C), 81.5 (C), 112.3 (CH), 112.9 (C), 114.0 (C), 119.1 (CH), 123.2 (CH), 123.3 (CH), 125.5 (CH), 125.6 (C), 126.1 (CH), 126.9 (CH), 127.8 (CH), 130.2 (C), 131.1 (CH), 140.4 (C), 142.4 (C), 142.9 (C), 143.7 (C), 146.2 (C), 150.1 (C), 150.5 (C), 158.3 (CH). Anal. Calcd for C₃₆H₂₅N₃S·(H₂O)_{0.24}: C, 80.67; H, 4.79; N, 7.84. Found: C, 80.71; H, 4.69; N, 7.73 (The analytical sample was dried at 160 °C in vacuo for 3 days, but the amount (0.24) of H₂O still remained. The amount of H₂O was determined as similarly as the case of **3d**).

■ ASSOCIATED CONTENT

Supporting Information

The Supporting Information is available free of charge on the ACS Publications website at DOI: 10.1021/acs.joc.5b02189.

ORTEP drawing, tables of selected bond length and bond angle data for **3** and **4**, optical absorption and emission spectra of **3** and **4**, Lippert–Mataga plots for **3** and **4**, cyclic voltammograms for **3** and **4**, computational

details for **3d** and **4d**, and ¹H NMR and ¹³C NMR spectra of all of products (PDF)

X-ray crystallographic data for **3a** (CIF)

X-ray crystallographic data for **3b** (CIF)

X-ray crystallographic data for **3c** (CIF)

X-ray crystallographic data for **3d** (CIF)

X-ray crystallographic data for **4b** (CIF)

X-ray crystallographic data for **4c** (CIF)

X-ray crystallographic data for **4d** (CIF)

■ AUTHOR INFORMATION

Corresponding Author

*E-mail: ishiaki@chem.saitama-u.ac.jp.

Notes

The authors declare no competing financial interest.

■ REFERENCES

- (1) For reviews: (a) Yao, J.; Yang, M.; Duan, Y. *Chem. Rev.* **2014**, *114*, 6130–6178. (b) Pitchaiya, S.; Heinicke, L. A.; Custer, T. C.; Walter, N. G. *Chem. Rev.* **2014**, *114*, 3224–3265. (c) Escobedo, J. O.; Rusin, O.; Lim, S.; Strongin, R. M. *Curr. Opin. Chem. Biol.* **2010**, *14*, 64–70. (d) Kiyose, K.; Kojima, H.; Nagano, T. *Chem.–Asian J.* **2008**, *3*, 506–515. (e) Zheng, Q.; Juette, M. F.; Jockusch, S.; Wasserman, M. R.; Zhou, Z.; Altman, R. B.; Blanchard, S. C. *Chem. Soc. Rev.* **2014**, *43*, 1044–1056.
- (2) For recent papers: (a) Pastierik, T.; Šebej, P.; Medalová, J.; Štacko, P.; Klán, P. *J. Org. Chem.* **2014**, *79*, 3374–3382. (b) Zhang, X.; Yu, J.; Rong, Y.; Ye, F.; Chiu, D. T.; Uvdal, K. *Chem. Sci.* **2013**, *4*, 2143–2151. (c) Holzhauser, C.; Wagenknecht, H.-A. *J. Org. Chem.* **2013**, *78*, 7373–7379. (d) Sakamoto, N.; Ikeda, C.; Yamamura, M.; Nabeshima, T. *Chem. Commun.* **2012**, *48*, 4818–4820. (e) Niko, Y.; Moritomo, H.; Sugihara, H.; Suzuki, Y.; Kawamata, J.; Konishi, G.-i. *J. Mater. Chem. B* **2015**, *3*, 184–190.
- (3) Qian, G.; Wang, Z. Y. *Chem.–Asian J.* **2010**, *5*, 1006–1029.
- (4) (a) Cheng, X.; Li, D.; Zhang, Z.; Zhang, H.; Wang, Y. *Org. Lett.* **2014**, *16*, 880–883. (b) Shimizu, M.; Kaki, R.; Takeda, Y.; Hiyama, T.; Nagai, N.; Yamagishi, H.; Furutani, H. *Angew. Chem., Int. Ed.* **2012**, *51*, 4095–4099. (c) D'Aléo, A.; Gachet, D.; Heresanu, V.; Giorgi, M.; Fages, F. *Chem.–Eur. J.* **2012**, *18*, 12764–12772.
- (5) (a) Biegger, P.; Stolz, S.; Intorp, S. N.; Zhang, Y.; Engelhart, J. U.; Rominger, F.; Hardcastle, K. I.; Lemmer, U.; Qian, X.; Hamburger, M.; Bunz, U. H. F. *J. Org. Chem.* **2015**, *80*, 582–589. (b) Wolak, M. A.; Melinger, J. S.; Lane, P. A.; Palilis, L. C.; Landis, C. A.; Delcamp, J.; Anthony, J. E.; Kafafi, Z. H. *J. Phys. Chem. B* **2006**, *110*, 7928–7937. (c) Picciolo, L. C.; Murata, H.; Kafafi, Z. H. *Appl. Phys. Lett.* **2001**, *78*, 2378–2380.
- (6) (a) Zhao, D.; Swager, T. M. *Org. Lett.* **2005**, *7*, 4357–4360. (b) Thomas, S. W., III; Joly, G. D.; Swager, T. M. *Chem. Rev.* **2007**, *107*, 1339–1386. (c) Esser, B.; Swager, T. M. *Angew. Chem., Int. Ed.* **2010**, *49*, 8872–8875. (d) Cox, J. R.; Müller, P.; Swager, T. M. *J. Am. Chem. Soc.* **2011**, *133*, 12910–12913. (e) Andrew, T. L.; Swager, T. M. *J. Polym. Sci., Part B: Polym. Phys.* **2011**, *49*, 476–498.
- (7) (a) Tan, W. S.; Prabhakar, Ch.; Liu, Y.-H.; Peng, S.-M.; Yang, J.-S. *Photochem. Photobiol. Sci.* **2014**, *13*, 211–223. See also: (b) Yang, J.-S.; Lin, C.-S.; Hwang, C.-Y. *Org. Lett.* **2001**, *3*, 889–892. (c) Yang, J.-S.; Yan, J.-L.; Lin, C.-K.; Chen, C.-Y.; Xie, Z.-Y.; Chen, C.-H. *Angew. Chem., Int. Ed.* **2009**, *48*, 9936–9939.
- (8) (a) Ishii, A.; Yamaguchi, Y.; Nakata, N. *Org. Lett.* **2011**, *13*, 3702–3705. (b) Ishii, A.; Annaka, T.; Nakata, N. *Chem.–Eur. J.* **2012**, *18*, 6428–6432. (c) Annaka, T.; Nakata, N.; Ishii, A. *Bull. Chem. Soc. Jpn.* **2015**, *88*, 554–561.
- (9) Ishii, A.; Aoki, Y.; Nakata, N. *J. Org. Chem.* **2014**, *79*, 7951–7960.
- (10) Ishii, A.; Kobayashi, S.; Aoki, Y.; Annaka, T.; Nakata, N. *Heteroat. Chem.* **2014**, *25*, 658–673.
- (11) Yamaguchi, Y.; Nakata, N.; Ishii, A. *Eur. J. Inorg. Chem.* **2013**, *2013*, 5233–5239.

(12) (a) Zyryanov, G. V.; Palacios, M. A.; Anzenbacher, P., Jr. *Org. Lett.* **2008**, *10*, 3681–3684. (b) Gu, X.; Lai, Y.-H. *Org. Lett.* **2010**, *12*, 5200–5203. (c) Hu, S.-Z.; Chen, C.-F. *Org. Biomol. Chem.* **2011**, *9*, 5838–5844.

(13) Shimizu, M.; Mochida, K.; Katoh, M.; Hiyama, T. *J. Phys. Chem. C* **2010**, *114*, 10004–10014.

(14) (a) Beinhoff, M.; Weigel, W.; Jurczok, M.; Rettig, W.; Modrakowski, C.; Brüdgam, L.; Hartl, H.; Schlüter, A. D. *Eur. J. Org. Chem.* **2001**, *2001*, 3819–3829. (b) Samori, S.; Tojo, S.; Fujitsuka, M.; Spitler, E. L.; Haley, M. M.; Majima, T. *J. Org. Chem.* **2007**, *72*, 2785–2793. (c) Agarwal, N.; Nayak, P. K.; Periasamy, N. *J. Chem. Sci.* **2008**, *120*, 355–362.

(15) Except for **3b** and **4b**, Φ_F decreased extremely in MeOH, implying the presence of a strong specific intermolecular interaction between the solvent molecules and substances. Therefore, the data in MeOH were excluded from the following discussion, although the data are listed in tables in the [Supporting Information](#).

(16) Reichardt, C.; Welton, T. In *Solvents and Solvent Effects in Organic Chemistry*, 4th ed.; Wiley-VCH Verlag GmbH & Co. KGaA: Weinheim, 2011; p 393. (b) Strehmel, B.; Sarker, A. M.; Malpert, J. H.; Strehmel, V.; Seifert, H.; Neckers, D. C. *J. Am. Chem. Soc.* **1999**, *121*, 1226–1236. (c) Krebs, F. C.; Spanggaard, H. *J. Org. Chem.* **2002**, *67*, 7185–7192. (d) Zhao, C.-H.; Sakuda, E.; Wakamiya, A.; Yamaguchi, S. *Chem.–Eur. J.* **2009**, *15*, 10603–10612.

(17) Reichardt, C.; Welton, T. In *Solvents and Solvent Effects in Organic Chemistry*, 4th ed.; Wiley-VCH Verlag GmbH & Co. KGaA: Weinheim, 2011; p 374.

(18) (a) Domínguez, M.; Rezende, M. C. *J. Phys. Org. Chem.* **2010**, *23*, 156–170. (b) Rezende, M. C.; Aracena, A. *Chem. Phys. Lett.* **2013**, *558*, 77–81. (c) Catalán, J. *Dyes Pigm.* **2012**, *95*, 180–187. (d) Botrel, A.; Aboab, B.; Corre, F.; Tonnard, F. *Chem. Phys.* **1995**, *194*, 101–116. (e) Shafeekh, K. M.; Das, S.; Sissa, C.; Painelli, A. *J. Phys. Chem. B* **2013**, *117*, 8536–8546.

(19) (a) Zhou, X.-H.; Luo, J.; Davies, J. A.; Huang, S.; Jen, A. K. Y. *J. Mater. Chem.* **2012**, *22*, 16390–16398. (b) de Melo, C. E. A.; Nandi, L. G.; Domínguez, M.; Rezende, M. C.; Machado, V. G. *J. Phys. Org. Chem.* **2015**, *28*, 250–260. (c) Rieth, T.; Marszalek, T.; Pisula, W.; Detert, H. *Chem.–Eur. J.* **2014**, *20*, 5000–5006. (d) Domagalska, B. W.; Wilk, K. A.; Zielinski, R. *J. Photochem. Photobiol., A* **2006**, *184*, 193–203. (e) Würthner, F.; Archetti, G.; Schmidt, R.; Kuball, H.-G. *Angew. Chem., Int. Ed.* **2008**, *47*, 4529–4532.

(20) La Clair, J. J. *Angew. Chem., Int. Ed.* **1998**, *37*, 325–329.

(21) Frisch, M. J.; Trucks, G. W.; Schlegel, H. B.; Scuseria, G. E.; Robb, M. A.; Cheeseman, J. R.; Scalmani, G.; Barone, V.; Mennucci, B.; Petersson, G. A.; Nakatsuji, H.; Caricato, M.; Li, X.; Hratchian, H. P.; Izmaylov, A. F.; Bloino, J.; Zheng, G.; Sonnenberg, J. L.; Hada, M.; Ehara, M.; Toyota, K.; Fukuda, R.; Hasegawa, J.; Ishida, M.; Nakajima, T.; Honda, Y.; Kitao, O.; Nakai, H.; Vreven, T.; Montgomery, J. A., Jr.; Peralta, J. E.; Ogliaro, F.; Bearpark, M.; Heyd, J. J.; Brothers, E.; Kudin, K. N.; Staroverov, V. N.; Keith, T.; Kobayashi, R.; Normand, J.; Raghavachari, K.; Rendell, A.; Burant, J. C.; Iyengar, S. S.; Tomasi, J.; Cossi, M.; Rega, N.; Millam, J. M.; Klene, M.; Knox, J. E.; Cross, J. B.; Bakken, V.; Adamo, C.; Jaramillo, J.; Gomperts, R.; Stratmann, R. E.; Yazyev, O.; Austin, A. J.; Cammi, R.; Pomelli, C.; Ochterski, J. W.; Martin, R. L.; Morokuma, K.; Zakrzewski, V. G.; Voth, G. A.; Salvador, P.; Dannenberg, J. J.; Dapprich, S.; Daniels, A. D.; Farkas, O.; Foresman, J. B.; Ortiz, J. V.; Cioslowski, J.; Fox, D. J. *Gaussian 09*, Revision D.01; Gaussian, Inc.: Wallingford, CT, 2013.

(22) HOMO levels were obtained with oxidation potentials measured by cyclic voltammetry in CH₂Cl₂, and LUMO levels were estimated with values of the HOMO levels and HOMO–LUMO gaps estimated from the edges of the long-wavelength absorptions in CH₂Cl₂ (see the [Supporting Information](#), Figures S15–S18 and Tables S14 and S15).